20. H. Yamamoto *et al.*, *J. Immunol.* **145**, 3740 (1990).
21. L. Shen, unpublished data.
22. G. Mazzara, unpublished data.
23. Recombinant protein SIV_{mac} gp140 was provided by S. Putney (Repligen, Cambridge, MA).
24. J. R. Bennink *et al.*, *Nature* **311**, 578 (1984).
25. E. McLaughlin-Taylor *et al.*, *J. Gen. Virol.* **69**, 1731 (1988).
26. P. L. Earl *et al.*, *Science* **234**, 728 (1986).
27. F. Michel *et al.*, *Eur. J. Immunol.* **18**, 1917 (1988).
28. D. Zagury *et al.*, *Nature* **332**, 728 (1988).
29. R. J. Orentas *et al.*, *Science* **248**, 1234 (1990).
30. J. M. Zarling *et al.*, *J. Immunol.* **139**, 988 (1987).
31. P. Doherty and R. Zinkernagel, *Transplant. Rev.* **19**, 89 (1974).
32. Abbreviations for the amino acid residues are as follows: A, Ala; C, Cys; D, Asp; E, Glu; F, Phe; G, Gly; H, His; I, Ile; K, Lys; L, Leu; M. Met; N, Asn; P, Pro; Q, Gln; R, Arg; S, Ser; T, Thr; V, Val; W, Trp; and Y, Tyr.
33. Monoclonal antibodies were provided by S. Schlossman (Dana-Farber Cancer Institute, Boston, MA).
34. We thank G. Hwang and D. Brosseau for help in manuscript preparation. Supported by NIH grants AI20729, CA50139, and AI26507 and by Division of Research Resources grant RR00168. N.L.L. is a recipient of an American Cancer Society Faculty Research Award.

19 September 1990; accepted 24 January 1991

Calcium as a Coagonist of Inositol 1,4,5-Trisphosphate–Induced Calcium Release

ELIZABETH A. FINCH, TIMOTHY J. TURNER, STANLEY M. GOLDIN*

Inositol 1,4,5-trisphosphate (IP_3)–induced calcium release from intracellular stores is a regulator of cytosolic-free calcium levels. The subsecond kinetics and regulation of IP_3-induced calcium-45 release from synaptosome-derived microsomal vesicles were resolved by rapid superfusion. Extravesicular calcium acted as a coagonist, potentiating the transient IP_3-induced release of calcium-45. Thus, rapid elevation of cytosolic calcium levels may trigger IP_3-induced calcium release in vivo. Extravesicular calcium also produced a more slowly developing, reversible inhibition of IP_3-induced calcium-45 release. Sequential positive and negative feedback regulation by calcium of IP_3-induced calcium release may contribute to transients and oscillations of cytosolic-free calcium in vivo.

A VARIETY OF EXTRACELLULAR SIGnals regulate intracellular processes by triggering increases in cytosolic Ca^{2+} concentration. Such increases are produced by entry of Ca^{2+} across the plasma membrane or release of Ca^{2+} from intracellular stores, or both. IP_3 is a phospholipid metabolite that couples the activation of cell surface receptors to changes in intracellular Ca^{2+} concentration by stimulating Ca^{2+} release from intracellular stores (*1*). An IP_3 receptor from mammalian brain has been purified (*2*), cloned (*3*), and reconstituted in lipid vesicles (*4*), and it appears that the IP_3 binding site and the Ca^{2+} release channel reside in a single protein. Elevation of cytosolic or extravesicular Ca^{2+} (Ca_e^{2+}) inhibits IP_3-induced Ca^{2+} release (*5*). To clarify the relationship between Ca_e^{2+} and the IP_3 receptor, we used a rapid superfusion system (*6*) to study $^{45}Ca^{2+}$ release from microsomal vesicles derived from rat brain synaptosomes, a nerve terminal preparation.

Microsomal vesicles were obtained by hypotonic lysis and discontinuous sucrose gradient centrifugation of rat brain synaptosomes (*7*). This resulted in six fractions, two of which (D and E) released accumulated $^{45}Ca^{2+}$ when exposed to IP_3. Fraction D was more active and was chosen for further characterization.

The vesicles actively accumulated $^{45}Ca^{2+}$ in an adenosine triphosphate (ATP)–dependent manner (*8*), and were retained on filters in a superfusion chamber accessed by three solenoid-driven valves that were operated by computer (*6*). Each valve controlled the delivery of a separate pressurized solution to the chamber. The $^{45}Ca^{2+}$ containing effluent was continuously collected by a high-speed fraction collector. The high flow rate (1 to 2 ml/s) relative to the small dead volume of the superfusion chamber (30 μl) allowed rapid solution changes and precise control of the extravesicular concentrations of IP_3 and Ca^{2+} (*9*), and afforded a time resolution ≤70 ms (*6*). The resulting rapid removal of released $^{45}Ca^{2+}$ isolated the efflux from other processes, such as reuptake, Ca^{2+} buffering, and agonist depletion. Thus, the effects of various agents on release could be readily quantified.

Continuous superfusion of vesicles with IP_3 resulted in a transient release of $^{45}Ca^{2+}$ (Fig. 1A). Vesicles were initially superfused with a buffer containing 100 nM Ca^{2+}, and $^{45}Ca^{2+}$ release was evoked by superfusion with a buffer containing 1 μM IP_3 and 10 μM Ca^{2+}. The release rate (*10*) reached a maximum within 140 ms after introduction of IP_3 and decayed exponentially over the next second (*11*). The IP_3-stimulated release was blocked by heparin (100 μg/ml), which inhibits the binding of IP_3 to its receptor (*2*). There was an additional smaller and kinetically distinct component of $^{45}Ca^{2+}$ release, stimulated by Ca_e^{2+} alone. It was not sensitive to heparin, but was nearly completely blocked by 3 to 5 mM Mg^{2+} (Fig. 1B). At ≤5 mM, Mg^{2+} had no effect on net $^{45}Ca^{2+}$ release evoked by 1 μM IP_3 [calculated as described in (*12*)]. The selective block of the IP_3-induced $^{45}Ca^{2+}$ release by heparin and the Ca_e^{2+}-mediated component of $^{45}Ca^{2+}$ release by Mg^{2+} suggested that each of these processes was mediated by an independent release mechanism and provided pharmacological criteria for distinguishing them (*12*).

The dependence on IP_3 concentration of the maximum observed rate of net $^{45}Ca^{2+}$ release (*12*) (Fig. 2) indicated that IP_3 concentration and $^{45}Ca^{2+}$ release rate were related in a normal hyperbolic manner over the range of 30 nM to 10 μM. The Hill coefficient (n_H) ± SD was 1.0 ± 0.2, and the half-maximal concentration (EC_{50}) was 240 ± 60 nM (Fig. 2, inset). At saturating IP_3 concentrations (10 μM), only 6% of the total accumulated $^{45}Ca^{2+}$ was released during the 2-s stimulus, whereas all of the $^{45}Ca^{2+}$ was discharged by the Ca^{2+} ionophore A23187 (1 μM).

We then explored possible explanations for the transient nature of the IP_3-evoked $^{45}Ca^{2+}$ release. If decay was due to depletion of releasable $^{45}Ca^{2+}$, the total amount of isotope released would have been the same for all IP_3 concentrations, but the rate of decay would have increased at higher agonist concentrations (Fig. 2). In contrast, the amount of $^{45}Ca^{2+}$ released increased as a function of IP_3 concentration (Fig. 2, inset), whereas the time constant for decay of the $^{45}Ca^{2+}$ release was constant for each Ca_e^{2+} concentration (*13*). Gramicidin D (300 nM), a monovalent cation ionophore used to collapse a transmembrane electrostatic gradient that might develop from a net efflux of cations, did not alter the kinetics of $^{45}Ca^{2+}$ release (*14*). These observations suggested that receptor inactivation, rather than depletion of intravesicular $^{45}Ca^{2+}$ or electrostatic forces, accounted for the rapid decay of the $^{45}Ca^{2+}$ release.

The magnitude and the time course of IP_3-induced $^{45}Ca^{2+}$ release were modulated

E. A. Finch, Program in Neuroscience, Department of Neurobiology, Harvard Medical School, Boston, MA 02115, and Cambridge Neuroscience Research, Inc., One Kendall Square, Building 700, Cambridge, MA 02139.
T. J. Turner, Department of Physiology, Tufts University School of Medicine, Boston, MA 02111.
S. M. Goldin, Cambridge Neuroscience Research, Inc., One Kendall Square, Building 700, Cambridge, MA 02139, and Department of Biological Chemistry and Molecular Pharmacology, Harvard Medical School, Boston, MA 02115.

*To whom correspondence should be addressed.

by Ca_e^{2+}. IP_3 (1 μM) was introduced in the presence of various Ca_e^{2+} concentrations (100 nM to 3 μM). Elevation of the Ca_e^{2+} concentration above 100 nM potentiated the maximum rate of IP_3-induced $^{45}Ca^{2+}$ release (Fig. 3A). The n_H for the potentiation by Ca_e^{2+} was 1.0 ± 0.02, and the EC_{50} was 660 ± 2 nM. The IP_3-induced $^{45}Ca^{2+}$ release rate, plotted as a function of Ca_e^{2+} concentration, extrapolated to zero at or below 60 nM Ca_e^{2+} (Fig. 3A, inset) (*15*). The requirement for both Ca_e^{2+} and IP_3 to evoke rapid, transient $^{45}Ca^{2+}$ release indicated that Ca^{2+} is a coagonist for IP_3 receptor activation.

The effect of increases in Ca_e^{2+} concentration at a constant IP_3 concentration provided additional evidence for a potentiating role of Ca_e^{2+}. In the continued presence of IP_3, an increase in Ca_e^{2+} concentration to 250 nM, and then a second step to 1 μM, resulted in two transients of $^{45}Ca^{2+}$ release corresponding to the Ca^{2+} steps (Fig. 3B). This result implied that incremental increases in Ca_e^{2+} concentration may sustain and amplify Ca^{2+} release, suggesting a positive feedback role in vivo for cytosolic Ca^{2+} in potentiating IP_3-induced Ca^{2+} release.

At higher Ca_e^{2+} concentrations (10 to 100 μM), the maximum observed rate of $^{45}Ca^{2+}$ release was diminished (Fig. 3C) and the decay of release was more rapid (Fig. 3A) (*13*), resulting in decreased cumulative $^{45}Ca^{2+}$ release (Fig. 3C). The biphasic Ca_e^{2+} concentration dependence suggested that there was a second, inhibitory effect of Ca_e^{2+}.

We further characterized the inhibitory effect of Ca_e^{2+} by giving a conditioning pulse with elevated Ca_e^{2+} concentration in the absence of IP_3 before a test pulse with a buffer containing 1 μM IP_3 and 10 μM Ca_e^{2+} (Fig. 4A). The 1-s conditioning pulse inhibited the subsequent IP_3 response in a concentration-dependent manner (*16*), with a concentration for 50% inhibition of cumulative $^{45}Ca^{2+}$ release (IC_{50}) of 620 ± 50 nM (Fig. 4B). These observations suggested that Ca_e^{2+} promoted inactivation of the release mechanism, independent of whether IP_3 was bound to the receptor. By varying the duration of the conditioning pulse, we determined the time constant for the onset of inhibition by 10 μM Ca_e^{2+} to be 580 ± 10 ms (Fig. 4C). The inhibition by Ca_e^{2+} was reversible (*17*): vesicles were pulsed with 10 μM Ca_e^{2+} for 1 s, then washed with 100 nM Ca_e^{2+} for various lengths of time to allow for recovery before a test pulse with 1 μM IP_3 and 10 μM Ca^{2+}. Approximately 50% of the release activity was recovered after 1 s of low–Ca_e^{2+} concentration wash. In the converse experiment, the response was not inhibited by a 1-s preexposure to 1 μM IP_3 at 100 nM Ca_e^{2+} (*17*). Thus, Ca_e^{2+}, but not IP_3, induced a reversible, concentration- and time-dependent inactivation of the release mechanism.

Our data show that Ca_e^{2+}, at physiological concentrations, rapidly activates and more slowly inactivates IP_3-induced Ca^{2+} release. Although the molecular mechanism underlying the potentiation by Ca^{2+} is unclear, an n_H of 1.0 is consistent with the existence of a regulatory Ca^{2+} binding site on the IP_3 receptor. The Ca_e^{2+}- and time-dependent control of the neuronal IP_3 receptor is similar to that described for the structurally homologous (*3*) ryanodine-sensitive Ca^{2+} release channels of sarcoplasmic reticulum (*18*).

In previous studies, Ca^{2+} was reported to inhibit IP_3-induced Ca^{2+} release (*5*), but the rapid potentiation by Ca_e^{2+} was not observed (*19*). Measurement of $^{45}Ca^{2+}$ efflux rates while maintaining constant Ca_e^{2+} and IP_3 concentrations allowed us to resolve and characterize the transient potentiation by Ca_e^{2+}. Our results explain the observations of Ca^{2+}-dependent inhibition (*5*) and the transient nature (*20, 21*) of IP_3-induced

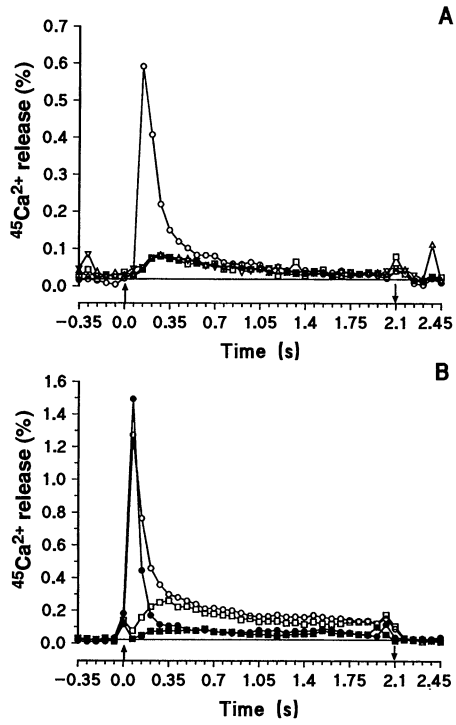

Fig. 1. Kinetic and pharmacological characteristics of IP_3-induced $^{45}Ca^{2+}$ release and Ca_e^{2+}-mediated $^{45}Ca^{2+}$ release activities from synaptosome-derived microsomal vesicles, fraction D. Vesicles were loaded with $^{45}Ca^{2+}$. The 3500-ms superfusion protocol consisted of a 750-ms superfusion with wash buffer, a 2000-ms superfusion with stimulation buffer, and another 750-ms superfusion with wash buffer. Upward arrow, switch to stimulation buffer (time = 0); downward arrow, switch to wash buffer. Wash buffer included 1 mM EGTA and 5 mM $MgCl_2$ (free Ca^{2+} concentration ≃ 100 nM). Stimulation buffer included 1 mM EGTA and was titrated with $CaCl_2$ to the desired free Ca^{2+} concentration, with or without IP_3 and other compounds, as described below. See (*6–9*) for experimental details. Each point represents the $^{45}Ca^{2+}$ content of a single superfusate fraction and corresponds to a 70-ms bin of $^{45}Ca^{2+}$ efflux. $^{45}Ca^{2+}$ release in these and subsequent experiments is expressed as percent of the total $^{45}Ca^{2+}$ accumulated by the vesicles that is released in each fraction (*10*), and thus is a measure of the average rate of $^{45}Ca^{2+}$ efflux during that 70-ms period. (**A**) Superfusion of vesicles with 10 μM Ca^{2+} (□); 10 μM Ca^{2+} plus 1 μM IP_3 (○); 10 μM Ca^{2+} plus heparin (100 μg/ml) in loading, wash, and stimulation buffer (△); and 10 μM Ca^{2+} plus 1 μM IP_3 plus heparin (▽). Heparin did not affect ATP-dependent $^{45}Ca^{2+}$ uptake during vesicle loading (*17*). (**B**) Superfusion of vesicles with 10 μM Ca^{2+} (□), 10 μM Ca^{2+} plus 5 mM Mg^{2+} (■), 10 μM Ca^{2+} plus 1 μM IP_3 (○), and 10 μM Ca^{2+} plus 1 μM IP_3 plus 5 mM Mg^{2+} (●).

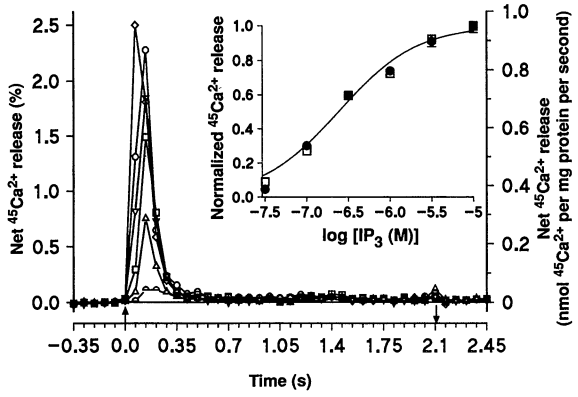

Fig. 2. Dependence of $^{45}Ca^{2+}$ efflux on IP_3 concentration. At time = 0, 10 μM Ca^{2+} and 0.03 (semicircle), 0.1 (△), 0.3 (□), 1 (▽), 3 (○), or 10 (◇) μM IP_3 was introduced. The superfusion protocol was as in Fig. 1. Data is shown as net IP_3-dependent $^{45}Ca^{2+}$ release (*12*), and is displayed as both percent of total $^{45}Ca^{2+}$ released in each 70-ms fraction (left ordinate) and as nanomoles of $^{45}Ca^{2+}$ per milligram of protein per second (right ordinate) (*10*). Data are averages of two experiments at each IP_3 concentration. (**Inset**) The maximum observed rate of $^{45}Ca^{2+}$ efflux (●) and cumulative amount of $^{45}Ca^{2+}$ efflux (□) as a function of IP_3 concentration. The data are normalized, with release at 10 μM IP_3 as 1.0. Ranges are shown when not smaller than the symbol. The correspondence between the normalized maximum release rate (n_H = 1.0 ± 0.2, EC_{50} = 240 ± 60 nM) and cumulative release measurements (n_H = 0.9 ± 0.2, EC_{50} = 270 ± 70 nM) corroborate the invariance of decay constant as a function of IP_3 concentration (*13*). The IP_3 dependence of $^{45}Ca^{2+}$ efflux was also determined in separate experiments with 1 μM Ca^{2+} (n_H = 0.80 ± 0.2 for maximum rate and 1.0 ± 0.002 for cumulative release) (*17*).

Ca^{2+} release by demonstrating that release inactivates with time and that the time course of inactivation is dependent on Ca_e^{2+} concentration. Consequently, a small and Ca_e^{2+}-dependent fraction of the stored $^{45}Ca^{2+}$ is released during superfusion. The fraction of total Ca^{2+} stores released by IP_3 is comparable to that observed from neural [Jean and Klee, in (*5*)] and hepatocyte (*20*) microsomes but is smaller than that described in some studies of permeabilized cells (*20, 21*). These differences could be due to experimental conditions or to tissue-specific differences in the relative amounts of IP_3-sensitive and IP_3-insensitive Ca^{2+} stores.

Although we obtained a normal hyperbolic relationship between IP_3 concentration and $^{45}Ca^{2+}$ release, some studies have reported positive cooperativity (*20, 21*). This could be because, in a permeabilized cell system, diffusion barriers produce a local increase in Ca_e^{2+} concentration due to Ca^{2+} release. The predicted positive feedback loop by Ca_e^{2+} could produce a steep IP_3 concentration–response relationship. Alternatively, regulation of the neuronal IP_3 receptor may differ from that of peripheral subtypes.

Sequential positive and negative feedback regulation of IP_3-induced Ca^{2+} release by Ca_e^{2+} may contribute to the generation of cytosolic Ca^{2+} transients in neurons as in Ca^{2+}-induced Ca^{2+} release from sarcoplasmic reticulum (*18*) and could contribute to the regulation of IP_3-induced Ca^{2+} oscillations by Ca_e^{2+} (*22*). At constant IP_3 concentrations, an initial increase in local free Ca^{2+} concentrations could trigger IP_3-induced Ca^{2+} release (*23*). Sustained elevation of local cytosolic Ca^{2+} would inactivate the release process. The subsequent reduction in cytosolic Ca^{2+} effected by homeostatic mechanisms would enable recovery from inactivation, thus regenerating the release activity. Regulation by Ca_e^{2+} could be due to Ca^{2+} entry across the plasma membrane or release from internal stores, or both, suggesting additional complexity in the crosstalk among various Ca^{2+} signaling pathways. Moreover, if Ca^{2+} entry can trigger IP_3-induced Ca^{2+} release, then this internal store may contribute, more than has been appreciated, to increased cytosolic Ca^{2+} concentrations in response to activation of the *N*-methyl-D-aspartate (NMDA)–gated subclass of glutamate receptors or voltage-sensitive Ca^{2+} channels.

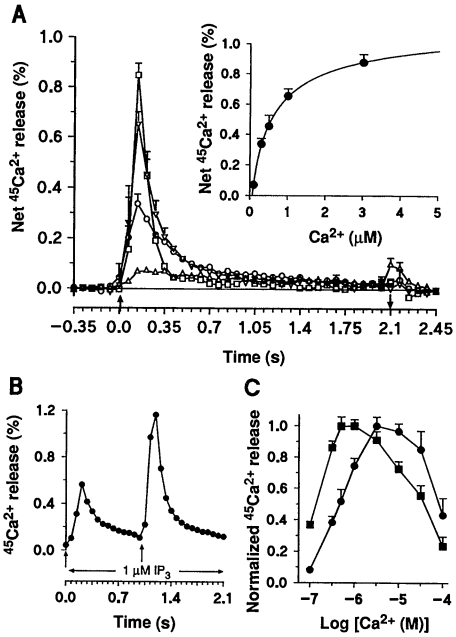

Fig. 3. Dependence of IP_3-induced $^{45}Ca^{2+}$ efflux on Ca_e^{2+} concentration. The IP_3 in the stimulation buffer was 1 μM. The range of Ca_e^{2+} concentrations in different experiments was 100 nM to 100 μM. Unless indicated otherwise, the superfusion protocol was as in Fig. 1. (**A**) Net IP_3-induced $^{45}Ca^{2+}$ efflux at 100 nM (△), 300 nM (○), 1 μM (▽), and 10 μM (□) Ca_e^{2+}. (**Inset**) Ca_e^{2+} dependence of the maximum rate of IP_3-induced $^{45}Ca^{2+}$ efflux, in the Ca_e^{2+} range where potentiation was observed. The curve is a linear plot of the least squares fit of the data to the Hill equation (*15*). (**B**) Multiple IP_3-induced $^{45}Ca^{2+}$ release events in response to step increases in Ca_e^{2+} concentration. Superfusion with 1 μM IP_3 was initiated at time = 0 and maintained throughout the period shown. Ca_e^{2+} was 250 nM for the first second of superfusion and was then increased to 1 μM (second vertical arrow). (**C**) Biphasic Ca_e^{2+} dependence of the maximum rate of (●) and cumulative amount of (■) $^{45}Ca^{2+}$ efflux over a 2-s superfusion period at various Ca_e^{2+} concentrations (100 nM to 100 μM). The data are normalized to the maximum value obtained for each of these measures. The data are from a series of experiments, a subset of which was used to generate (A). Data are the means ± SD for three to five separate experiments at each Ca_e^{2+} concentration. Error bars are not shown when smaller than the symbol.

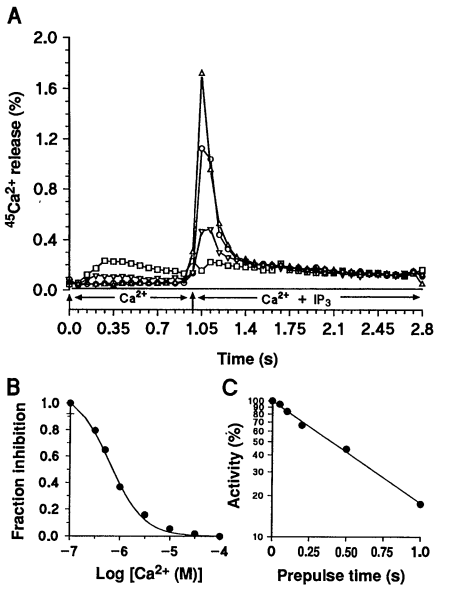

Fig. 4. Ca_e^{2+}- and time-dependent inactivation of IP_3–induced $^{45}Ca^{2+}$ release. (**A**) Exposure to Ca_e^{2+} inhibited subsequent IP_3-induced $^{45}Ca^{2+}$ efflux. After a 350-ms superfusion with wash buffer, vesicles were exposed at time = 0 to a 1-s conditioning pulse of stimulation buffer containing 100 nM (△), 300 nM (○), 1 μM (▽), and 10 μM (□) Ca^{2+}. Subsequently (second vertical arrow), a standard 2-s test pulse with stimulation buffer containing 1 μM IP_3 and 10 μM Ca^{2+} was delivered. (**B**) Concentration-response relation for Ca_e^{2+}-dependent inactivation of IP_3-induced $^{45}Ca^{2+}$ release. The data represent cumulative $^{45}Ca^{2+}$ release from a series of experiments, a subset of which was used to generate (A) (n = 2 or 3 for each Ca_e^{2+} concentration). Error bars (± SD) are not shown when smaller than the symbol. (**C**) Rate of onset of inactivation to a prior 10 μM Ca_e^{2+} exposure. A protocol similar to that in (A) was used, but in this case the length of the conditioning pulse varied from 50 to 1000 ms. Data are plotted as the percentage of the control, which was the cumulative IP_3-induced $^{45}Ca^{2+}$ release obtained with no conditioning pulse. A time constant of 580 ± 10 ms was derived from the reciprocal of the slope of the regression line of the semilog plot.

REFERENCES AND NOTES

1. M. J. Berridge, *Annu. Rev. Biochem.* **56**, 159 (1987); R. F. Irvine, *Nature* **341**, 197 (1989).
2. S. Supattapone, P. F. Worley, J. M. Baraban, S. H. Snyder, *J. Biol. Chem.* **263**, 1530 (1988).
3. T. Furuichi *et al.*, *Nature* **342**, 32 (1989); G. A. Mignery, T. C. Sudhof, K. Takei, P. de Camilli, *ibid.*, p. 192.
4. C. D. Ferris, R. L. Huganir, S. Supattapone, S. H. Snyder, *ibid.*, p. 87.
5. S.-H. Chueh and D. L. Gill, *J. Biol. Chem.* **261**, 13883 (1986); T. Jean and C. B. Klee, *ibid.*, p. 16414; J. Shah, R. S. Cohen, H. C. Pant, *Brain Res.* **419**, 1 (1987); S. K. Joseph, H. L. Rice, J. R. Williamson, *Biochem. J.* **258**, 261 (1989); R. Payne, T. M. Flores, A. Fein, *Neuron* **4**, 547 (1990); I. Parker and I. Ivorra, *Proc. Natl. Acad. Sci. U.S.A.* **87**, 260 (1990).
6. L. B. Pearce, R. D. Calhoon, P. R. Burns, A. Vincent, S. M. Goldin, *Biochemistry* **27**, 4396 (1988); T. J. Turner, L. B. Pearce, S. M. Goldin, *Anal. Biochem.* **178**, 8 (1989); T. J. Turner and S. M. Goldin, *Biochemistry* **28**, 586 (1989).
7. V. P. Whittaker, in *Handbook of Neurochemistry*, A. Lajtha, Ed. (Plenum, New York, 1969), vol. 2, pp. 327–364. Protease inhibitors (500 μg/ml EDTA, 0.5 μg/ml leupeptin, 0.7 μg/ml pepstatin, 100 μg/ml phenylmethylsulfonyl fluoride) were included in all steps. Subcellular fractions were diluted with basal buffer [20 mM MOPS (4-morpholinepropanesulfonic acid), 100 mM KCl, 10 mM NaCl, pH 7.2], pelleted, resuspended in basal buffer with 0.6 M glycerol, and stored at −60°C. The primary constituents of each fraction were determined by Whittaker to be D, synaptic vesicles; E, microsomes and some synaptic vesicles; F and G, synaptosome ghosts; H, partially disrupted synaptosomes; and I, mitochondria.
8. Vesicles (20 to 50 μg per 70 μl) were loaded with $^{45}Ca^{2+}$ by adding MgATP and $^{45}Ca^{2+}$ to final concentrations of 5 mM and 100 μM, respectively, and incubating at room temperature for 10 min, at which point a tenfold excess of wash buffer (basal buffer containing 1 mM EGTA and 5 mM $MgCl_2$) was added.
9. The Ca^{2+} concentration of the buffers was determined with a Phillips Ca^{2+}-selective electrode (Moller Glass-blowers, Zurich, Switzerland) and a Corning 0.1 M Ca^{2+} molarity standard. The response of

the electrode obeyed the Nernst equation at all Ca^{2+} concentrations.

10. $^{45}Ca^{2+}$ release rate is expressed as a percent of the total initial vesicular $^{45}Ca^{2+}$ content released in each fraction (*6*). Calculations normalized to percent of $^{45}Ca^{2+}$ released provided the most reproducible comparison of data between experiments. In Fig. 2, an additional ordinate is included that provides a less precise (±10%) approximation of the release rates as nanomoles of $^{45}Ca^{2+}$ per milligram of protein per second.
11. IP_3-induced $^{45}Ca^{2+}$ release decayed from its maximum rate with a time course that can be approximated by the sum of two first-order processes. The more rapidly decaying component predominated and is the basis for the majority of the analysis in this report.
12. Net IP_3-stimulated $^{45}Ca^{2+}$ release was the difference between $^{45}Ca^{2+}$ release at given IP_3 and Ca_c^{2+} concentrations and $^{45}Ca^{2+}$ release in the presence of the corresponding Ca_c^{2+} concentration alone. We did not use Mg^{2+} to differentiate the two components of release because the Mg^{2+} block was incomplete at higher Ca_c^{2+} concentrations.
13. Time constants for the rapid decay of $^{45}Ca^{2+}$ release were calculated for a range of IP_3 concentrations (100 nM to 10 μM) at a range of Ca_c^{2+} concentrations (300 nM to 10 μM). For a given Ca_c^{2+} concentration, the time constant for the more rapidly decaying component was constant (±10%) and ranged from 190 ms at 300 nM Ca_c^{2+} to ≤70 ms at or above 3 μM Ca_c^{2+}.
14. A. M. Garcia and C. Miller, *J. Gen. Physiol.* **83**, 819 (1984).
15. N. W. Kleckner and R. Dingledine, *Science* **241**, 835 (1988).
16. The diminished response to IP_3 after the Ca_c^{2+} conditioning pulse was not due to depletion of releasable $^{45}Ca^{2+}$, because 5 mM Mg^{2+} in the conditioning pulse buffer prevented $^{45}Ca^{2+}$ release during that pulse but did not alter the subsequent IP_3-induced $^{45}Ca^{2+}$ release.
17. E. A. Finch *et al.*, unpublished data.
18. A. Fabiato, *J. Gen. Physiol.* **85**, 247 (1985); G. Meissner, E. Darling, J. Eveleth, *Biochemistry* **25**, 236 (1986).
19. M. Iino [*J. Gen. Physiol.* **95**, 1103 (1990)] demonstrated a biphasic Ca_c^{2+} dependence at steady-state Ca_c^{2+} concentrations, with a maximum at 300 nM, but did not measure the subsecond kinetics of Ca^{2+} release.
20. P. Champeil *et al.*, *J. Biol. Chem.* **264**, 17665 (1989).
21. T. Meyer, D. Holowka, L. Stryer, *Science* **240**, 653 (1988); T. Meyer, T. Wensel, L. Stryer, *Biochemistry* **29**, 32 (1990); T. Meyer and L. Stryer, *Proc. Natl. Acad. Sci. U.S.A.* **87**, 3841 (1990).
22. R. Jacob, J. E. Merritt, T. J. Hallam, T. J. Rink, *Nature* **335**, 40 (1988); M. Wakui, B. V. L. Potter, O. H. Peterson, *ibid.* **339**, 317 (1989); M. J. Berridge and A. Galione, *FASEB J.* **2**, 3074 (1988); T. J. Rink and R. Jacob, *Trends Neurosci.* **12**, 43 (1989).
23. Y. Igusa and S.-I. Miyazaki, *J. Physiol.* **340**, 611 (1983); A. Fabiato, *J. Gen. Physiol.* **85**, 291 (1985); D. Lipscombe *et al.*, *Neuron* **1**, 355 (1988); M. Näbauer, G. Callewaert, L. Cleemann, M. Morad, *Science* **244**, 800 (1989); N. Leblanc and J. R. Hume, *ibid.* **248**, 372 (1990).
24. We thank J. Assad, B. Bean, E. Gamzu, P. Hess, A. Knapp, E. Kravitz, R. McBurney, C. Miller, K. Miller, and K. Sweadner for helpful comments; P. Hess for assistance with Ca^{2+} standard buffers; and B. McGowan for computer modeling of the data. Supported in part by NIH grant GM35423.

17 July 1990; accepted 1 February 1991

Primary Structure and Functional Activity of a Phosphatidylinositol-Glycan–Specific Phospholipase D

BERNARD J. SCALLON,* WEN-JIAN C. FUNG, T. CHRIS TSANG, SHIRLEY LI, HELEN KADO-FONG, KUO-SEN HUANG, JAREMA P. KOCHAN†

A phosphatidylinositol-glycan–specific phospholipase D (PI-G PLD) that specifically hydrolyzes the inositol phosphate linkage in proteins anchored by phosphatidylinositol-glycans (PI-Gs) has recently been purified from human and bovine sera. The primary structure of bovine PI-G PLD has now been determined and the functional activity of the enzyme has been studied. Expression of PI-G PLD complementary DNA in COS cells produced a protein that specifically hydrolyzed the inositol phosphate linkage of the PI-G anchor. Cotransfection of PI-G PLD with a PI-G–anchored protein resulted in the secretion of the PI-G–anchored protein. The results suggest that the expression of PI-G PLD may influence the expression and location of PI-G–anchored proteins.

THE ANCHORING OF PROTEINS TO the lipid bilayer of plasma membranes was initially thought to be mediated mainly by hydrophobic amino acid sequences. However, some proteins are covalently linked to a phosphatidylinositol-glycan (PI-G) molecule in the lipid bilayer (Fig. 1) (*1*). This structure has been shown to anchor numerous proteins in species as diverse as trypanosomes, schistosomes, mice, and humans (*1*). An enzyme has been identified that selectively hydrolyzes the inositol phosphate linkage of PI-G–anchored proteins, PI-G lipids, and related molecules (*2–5*). The enzyme, PI-G–specific phospholipase D (PI-G PLD), is abundant in serum and has been purified and characterized (*3, 4*). Purified PI-G PLD from serum can hydrolyze the inositol phosphate linkage of PI-G–anchored proteins in vitro in the presence of detergents (*2–5*). However, for reasons that are not understood, it has not been possible to release proteins with a PI-G anchor from the surface of intact cells using PI-G PLD (*2–4*).

On the basis of the amino acid sequences of eight tryptic fragments from bovine serum PI-G PLD (*3*), four degenerate oligonucleotide probes were made for the purpose of screening bovine DNA libraries for PI-G PLD DNA clones (*6*). A cDNA clone that predicted the exact amino acid sequence of all eight tryptic fragments was obtained. Comparison of the deduced protein sequence to the NH_2-terminal amino acid sequence of intact PI-G PLD revealed that the clone encoded the mature NH_2-terminus of the protein and that the translation product contained a signal peptide of 23 amino acids. A translation stop codon indicated that the gene encoded a mature protein of 817 amino acids (90.2 kD) with eight potential sites of N-linked glycosyla-

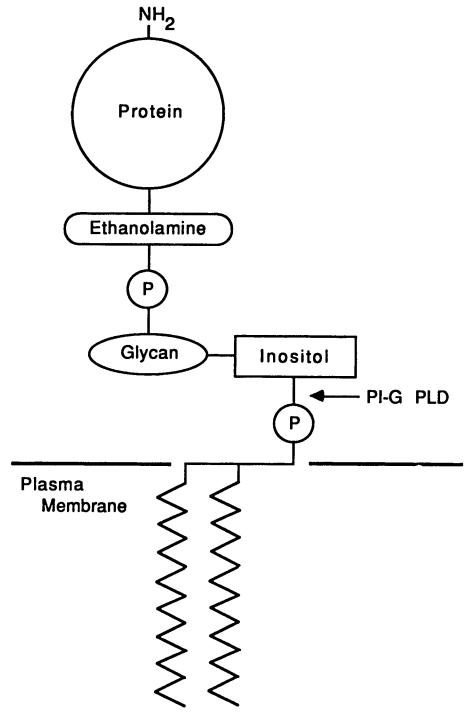

Fig. 1. Structure of the PI-G anchor. The COOH-terminal amino acid of the protein is linked to an ethanolamine residue which in turn is linked by a phosphodiester bond to a complex glycan moiety. In PI-G anchors studied in detail, such as variant surface glycoprotein from trypanosomes (*1*) and Thy-1 antigen from rat brain (*1*), the glycan is comprised of a mannose-mannose-mannose-glucosamine core structure with variable side chains. The glucosamine is linked to a membrane-anchored phosphatidylinositol. The site of PI-G PLD hydrolysis is marked.

Department of Molecular/Cellular Biology and Biochemistry, Hoffmann–La Roche, Inc., Nutley, NJ 07110.

*Present address: Department of Molecular Biology, Centocor, Inc., Malvern, PA 19355.
†To whom correspondence should be addressed.